Journal of MATERIALS RESEARCH

Article
DOI: 10.1557/jmr.2019.358

Antithrombotic, antimicrobial activities, and biocompatibility of surface-functionalized titanium

Guannan Zhang[1], Xingyu Zhang[1], Zhiping Sun[2], Xiaohong Yao[1,a)], Xiangyu Zhang[1,b)]

[1]College of Materials Science and Engineering, Taiyuan University of Technology, Taiyuan 030024, People's Republic of China
[2]School of Electromechanical and Automobile Engineering, Changzhou Vocational Institute of Engineering, Changzhou 213164, People's Republic of China

[a)]Address all correspondence to these authors. e-mail: xhyao@tyut.edu.cn
[b)]e-mail: zhangxiangyu@tyut.edu.cn

Received: 14 August 2019; accepted: 9 November 2019

Titanium (Ti) has been extensively used in medical devices owing to their low density, high strength, excellent corrosion resistance, and biocompatibility. However, thrombus formation and bacterial infections are still challenges for their application in specific clinical cases. Hence, we have developed a simple, efficient, and stable strategy that endow Ti with anticoagulant and antibacterial properties through chemical bonding and electrostatic bonding. A large number of hydroxyl groups were produced on the surface of Ti by annealing at 500 °C. Then, heparin was immobilized on annealed surface with chemical bonding and chitosan was captured in an electrostatically bound manner by simply soaking in solution. The results indicated that the surface-functionalized Ti exhibited excellent anticoagulant properties by a reduction in platelet adhesion and prolonged blood clotting time. Furthermore, the modified Ti also showed antibacterial properties against both *Escherichia coli* (*E. coli*) and *Staphylococcus aureus* (*S. aureus*).

Introduction

Thrombosis and bacterial infections are still the challenges restricting the applications of some medical devices, such as blood-contacting devices, biosensors, and drug delivery vehicle [1, 2, 3]. To address these problems, the surface modification of biomaterials by immobilization of biological molecules is becoming a topic of great interest [4, 5, 6, 7].

Titanium (Ti) has been widely used in medical devices due to its excellent performances. It was also known that the spontaneously formed TiO_2 film on Ti surfaces plays a major role in the corrosion resistance and biocompatibility [8, 9, 10, 11]. However, the thin spontaneously formed TiO_2 film can hardly maintain the long-term performances. Annealing is an effective and easy method to prepare relatively thick TiO_2 film on Ti [12, 13]. Beyond that, a large amount of hydroxyl radical (–OH) can be formed during the annealing treatment, which can build a bridge between biological molecules and Ti to immobilize them on the surface of Ti [14, 15, 16, 17].

As a common anticoagulant, heparin plays a key role in the coagulation process and can prolong the clotting time and prothrombin time. Lots of research has shown that heparin exhibited a rapid anticoagulant effect both in vivo and in vitro, mainly acting on fibrin and reducing platelet aggregation [18, 19, 20]. More importantly, heparin can covalently immobilize on the surface containing enormous amount of –OH of Ti. As a natural biopolymer with unique structure, chitosan exhibits a great potential for antibacterial properties [21, 22]. Many studies have demonstrated that chitosan exhibited excellent good antibacterial effect against a variety of bacteria [23, 24] and also possessed good biocompatibility [25, 26]. Beyond that, chitosan can be decomposed by the human body, avoiding the toxicity of common heavy metal element (e.g., Ag, Cu) [27, 28, 29]. Equally importantly, chitosan can immobilize on the heparinizing surfaces by electrostatic bonding.

In this work, we first propose a simple and stable tactics to impart antibacterial and antithrombotic properties to annealed Ti by synchronously immobilizing heparin and chitosan (Fig. 1). In order to verify the successful coimmobilization of heparin and chitosan, the modified surfaces were characterized by water-contact angle measurements, X-ray photoelectron spectroscopy (XPS), field-emission scanning electron microscopy (FE-SEM), and atomic force microscopy (AFM). The

https://doi.org/10.1557/jmr.2019.358 Published online by Cambridge University Press

© Materials Research Society 2019

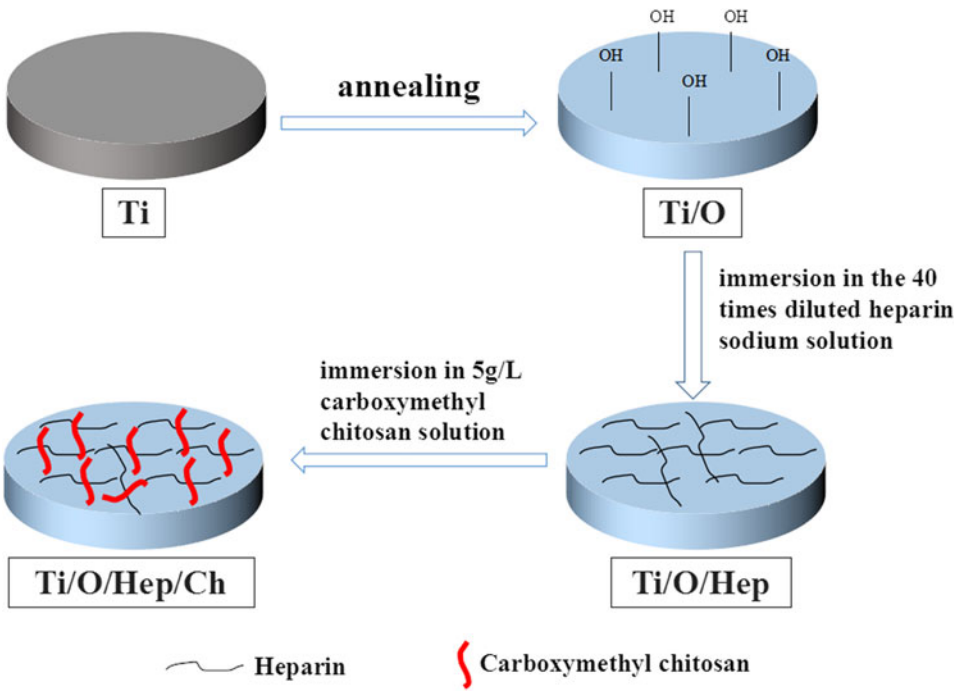


Figure 1: Schematic illustration of the synthetic route of the modified surfaces on Ti.

stability and the content of heparin in the surfaces were examined. The antithrombogenic properties were analyzed by platelet adhesion and blood clotting time. The antibacterial properties were analyzed by Live/Dead staining assay, spread plate analysis, and SEM observation.

Results and discussion

Sample characterization

Surface immobilization and characterization

The water contact angle was measured to characterize the wettability of the different samples [Fig. 2(a)]. The surface of Ti with a contact angle of 64.3°. The contact angle decreased dramatically to 25.7° for Ti/O on account of a good deal of hydroxyl groups on the sample surface formed during annealing treatment. After the sample was soaked in heparin solution, the contact angle increased to 43° for Ti/O/Hep. However, the contact angles of Ti/O/Hep/Ch1, Ti/O/Hep/Ch3, and Ti/O/Hep/Ch5 were 36.7°, 33.1°, and 31.5°, respectively, decreased again after repeated soaking in heparin and chitosan solutions at different times. Since the contact angle is related to the surface morphology and surface free energy, the result testified to the prosperous immobilization of heparin and chitosan molecules onto the Ti surface. From the quantitative results, the water contact angle of Ti/O/Hep/Ch3 and Ti/O/Hep/Ch5 was mildly lower than that of Ti/O/Hep/Ch1 immobilized surfaces and may be due to the fixed molecules that were reduced.

To further evaluate the changes in the surface of different samples, the amount of protein adsorbed on the surface of the samples after 4 h of culture in calf serum was measured. As shown in Fig. 2(b), all the treated specimens showed great resistance to protein adsorption compared to the Ti matrix. This result proved that surfaces with highly hydrophilic and different charged molecules such as heparin and chitosan decreased protein adsorption by reducing the hydrophobic and electrostatic interactions between the surface and protein, respectively [30]. This result also confirmed that heparin and chitosan were successfully fixed to the surface of the samples.

The surface chemical composition of Ti/O, Ti/O/Hep, and Ti/O/Hep/Ch1 was detected by XPS [Fig. 2(c)]. Compared with Ti/O, Ti/O/Hep and Ti/O/Hep/Ch1 showed a peak of sulfur (S 2*p*, 168 eV), which was derived from the heparin molecular sulfate group, confirming the successful immobilization of heparin on the Ti surface.

The surface morphology of each sample was characterized and analyzed by SEM and AFM. As shown in Fig. 2(d), the surface of Ti was generally smooth, while the modified surfaces were relatively coarse due to the annealing treatment. Nevertheless, no clear distinction could be searched out among Ti/O, Ti/O/Hep, Ti/O/Hep/Ch1 Ti/O/Hep/Ch3, and Ti/O/Hep/Ch5, confirming that the immobilization of heparin and chitosan had no effect on the surface morphology. The morphological difference was also confirmed by AFM and Fig. 2(e) shows that the root mean square (RMS) roughness increased drastically from 6.62 nm of Ti to 22 nm after annealing treatment. The

https://doi.org/10.1557/jmr.2019.358 Published online by Cambridge University Press

© Materials Research Society 2019

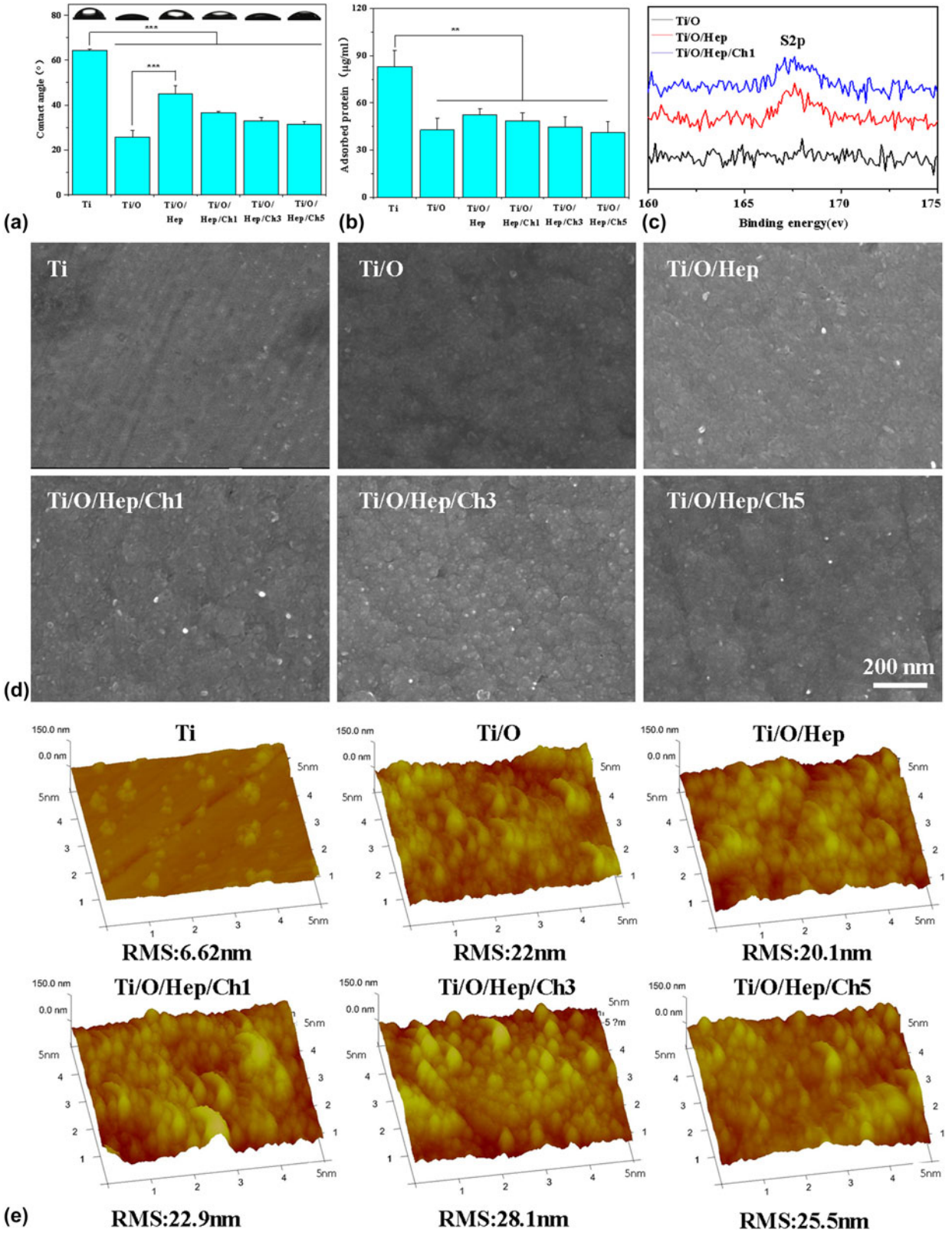


Figure 2: Characterization of Ti, Ti/O, Ti/O/Hep, Ti/O/Hep/Ch1, Ti/O/Hep/Ch3, and Ti/O/Hep/Ch5: (a) Water contact angle; (b) fibrinogen absorption; (c) XPS analysis; (d) SEM images; and (e) AFM images. (***$P < 0.001$, **$P < 0.01$)

https://doi.org/10.1557/jmr.2019.358 Published online by Cambridge University Press

© Materials Research Society 2019

results shown on the AFM images were basically the same as the SEM. The roughness did not significantly change after heparin and chitosan immobilizations.

Heparin sodium content and surface stability

The amount of heparin immobilized on surface was measured by the toluidine blue (TB) method (Fig. 3). The amount of heparin immobilized on Ti/O/Hep, Ti/O/Hep/Ch1, Ti/O/Hep/Ch3, and Ti/O/Hep/Ch5 was 0.092 μL/cm [2], 0.089 μL/cm [2], 0.08 μL/cm, and 0.075 μL/cm, respectively [2]. Further increased, the reaction time and polymer concentration did not significantly increase the amount of immobilized heparin. At the same time, the more times of repeated soaking, the heparin content decreased slightly. This is because the heparin content immobilized on Ti/O was not saturated in a short time and the surface was covered by chitosan in subsequent steps.

To evaluate the stability of heparin immobilization on the surface of the sample under physiological conditions, the samples were immersed in phosphate-buffered saline (PBS) for 10 and 20 days. As shown in Fig. 3, there was no significant change in the heparin amount detected for each sample. It may turn out that heparin was immobilized on the sample surface with high stability.

From the above results, we showed that the annealing is a brief and effective method to immobilize heparin onto Ti. Then the anticoagulant and antibacterial surfaces can be prepared by immobilizing chitosan through electrostatic binding onto the heparinization surfaces.

In vitro evaluation of antithrombogenicity

The formation of thrombus on the implant is a very complicated process. When the blood comes into contact with the implant, it activates the clotting factor and forms fibrin on the surface of the implant. At the same time, platelets adhere and aggregate on the implant surface, forming thrombus. Therefore, the anticoagulant properties of the samples are evaluated by the following experiments.

Whole blood clotting

The antithrombogenic activities of various samples were evaluated by blood clotting potential. When fresh blood was dropped onto the surfaces of the samples, they would form blood clot after a period of time, and the red blood cells will be trapped. Free red blood cells that were not trapped in the blood clot were dissolved by adding deionized water (DIW) and the hemoglobin was released. Therefore, the lost weight of whole blood after dissolved in DIW inversely relates to the blood clot size, and more weight lost values indicate greater thrombore-sistance. By the same token, the absorbance of hemoglobin

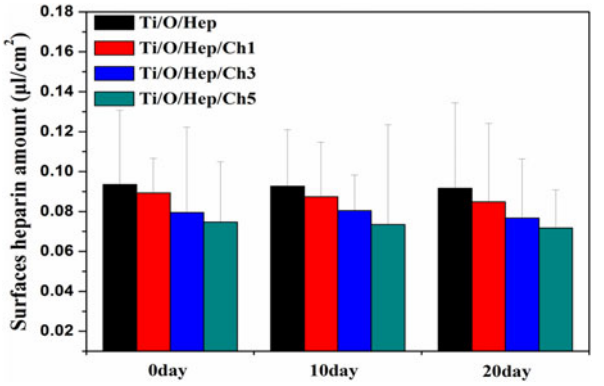


Figure 3: Heparin amounts on the Ti/O/Hep, Ti/O/Hep/Ch1, Ti/O/Hep/Ch3, and Ti/O/Hep/Ch5 after incubation in PBS for 0, 10, and 20 days.

released from free red blood cells was also inversely proportional to the size of blood clot. The higher the absorbance, the better the anticoagulant effect. Figures 4(a) and 4(b) show that the heparinized surfaces exhibited good anticoagulant efficacy compared with the substrate. This is because heparin can enhance the inhibitory effect of coagulation factors of (e.g., II, IX, X, XI, and XII) in the coagulation cascade [31, 32].

Platelet adhesion

Platelet adhesion is also a widely used method to test the antithrombotic properties of biomaterials. From the results of SEM images [Fig. 4(c)], the number of platelets adhered to the annealed specimens decreased slightly, and the amounts of adherent platelets on specimens can be further significantly reduced after surface heparinization. There was little difference in the number of platelet adhesions between Ti/O/Hep and Ti/O/Hep/Ch1, indicating that the antithrombogenic function of heparin was retained after linking with chitosan. For Ti/O/Hep/Ch3 and Ti/O/Hep/Ch5, the effect of antiplatelet adhesion gradually decreased due to the diminishing amount of heparin on the surfaces. It is believed that the immobilized heparin plays a major role in the antithrombogenic function. In addition, the hydrophilic surfaces also can suppress the platelet adhesion [33, 34].

Antibacterial properties

To evaluate the antibacterial activity of the specimens against *E. coli* and *S. aureus*, Live/Dead staining assay, spread plate analysis, and SEM observation were performed.

The results of Live/Dead two-color fluorescence were shown in Fig. 5. There were a large number of green spots on Ti, Ti/O, and Ti/O/Hep for both *E. coli* and *S. aureus*. On the contrary, the spots on the surfaces of Ti/O/Hep/Ch1, Ti/O/Hep/Ch3, and Ti/O/Hep/Ch5 were nearly all red. In order to further examine the bactericidal ability of the modified layer

https://doi.org/10.1557/jmr.2019.358 Published online by Cambridge University Press

© Materials Research Society 2019

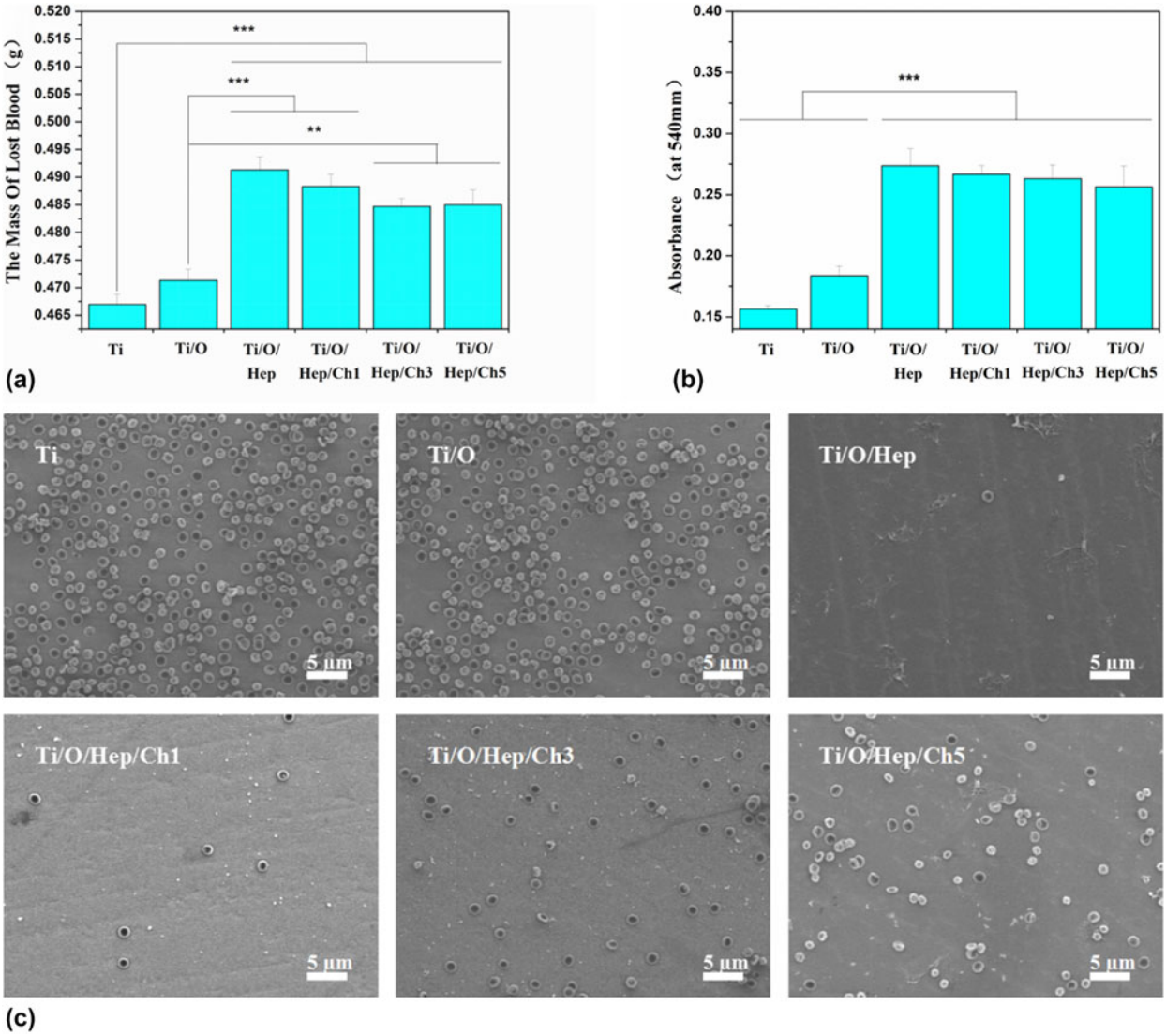


Figure 4: Antithrombotic effects: (a) Blood loss weight on samples after incubating with whole blood for 30 min; (b) the absorbance of hemolyzed hemoglobin solution; and (c) SEM images of platelet adhesion. (***$P < 0.001$, **$P < 0.01$)

against adherent bacteria, SEM analysis was performed again. The results shows that a large number of bacteria adhering on Ti, Ti/O, and Ti/O/Hep aggregate into clusters and reveal as smooth cell membrane surface, whereas those on the carboxymethyl chitosan (CMCS) immobilized Ti/O/Hep/Ch1, Ti/O/Hep/Ch3, and Ti/O/Hep/Ch5 exhibited withered, wrinkled, and even broken surfaces. The experimental characterizations have demonstrated that chitosan was successfully immobilized on the surface of the sample and showed excellent bactericidal effect on adherent bacteria.

Figure 5 also shows the representative photographs of the bacterial colonies on Ti, Ti/O, Ti/O/Hep, Ti/O/Hep/Ch1, Ti/O/Hep/Ch3, and Ti/O/Hep/Ch5. The bacterial colonies covered almost the entire agar plates corresponding to Ti, Ti/O, and Ti/O/Hep, indicating that the samples without immobilizing chitosan have no antibacterial function to planktonic bacteria. Compared with Ti, Ti/O, and Ti/O/Hep, the bacteria viability of Ti/O/Hep/Ch1, Ti/O/Hep/Ch3, and Ti/O/Hep/Ch5 was reduced by 56.5%, 57.8%, and 51.1% and 74.5%, 70.4%, and 68.9% for *E. coli* and *S. aureus*, respectively. The number of bacterial colonies significantly decreased on Ti/O/Hep/Ch1, Ti/O/Hep/Ch3, and Ti/O/Hep/Ch5, suggesting that the specimens with immobilizing chitosan also have bactericidal effect on planktonic bacteria. The figure also shows that the sterilization effect on *S. aureus* is better than the antibacterial function on *E. coli.* Many studies have shown that CMCS has excellent antibacterial properties, but the antibacterial mechanism is not the same for different bacteria. For *E. coli*, chitosan enters the cell, adsorbs negatively charged cytoplasm in the cell, disrupts normal cellular activity, and kills bacteria. For *S.*

https://doi.org/10.1557/jmr.2019.358 Published online by Cambridge University Press

© Materials Research Society 2019

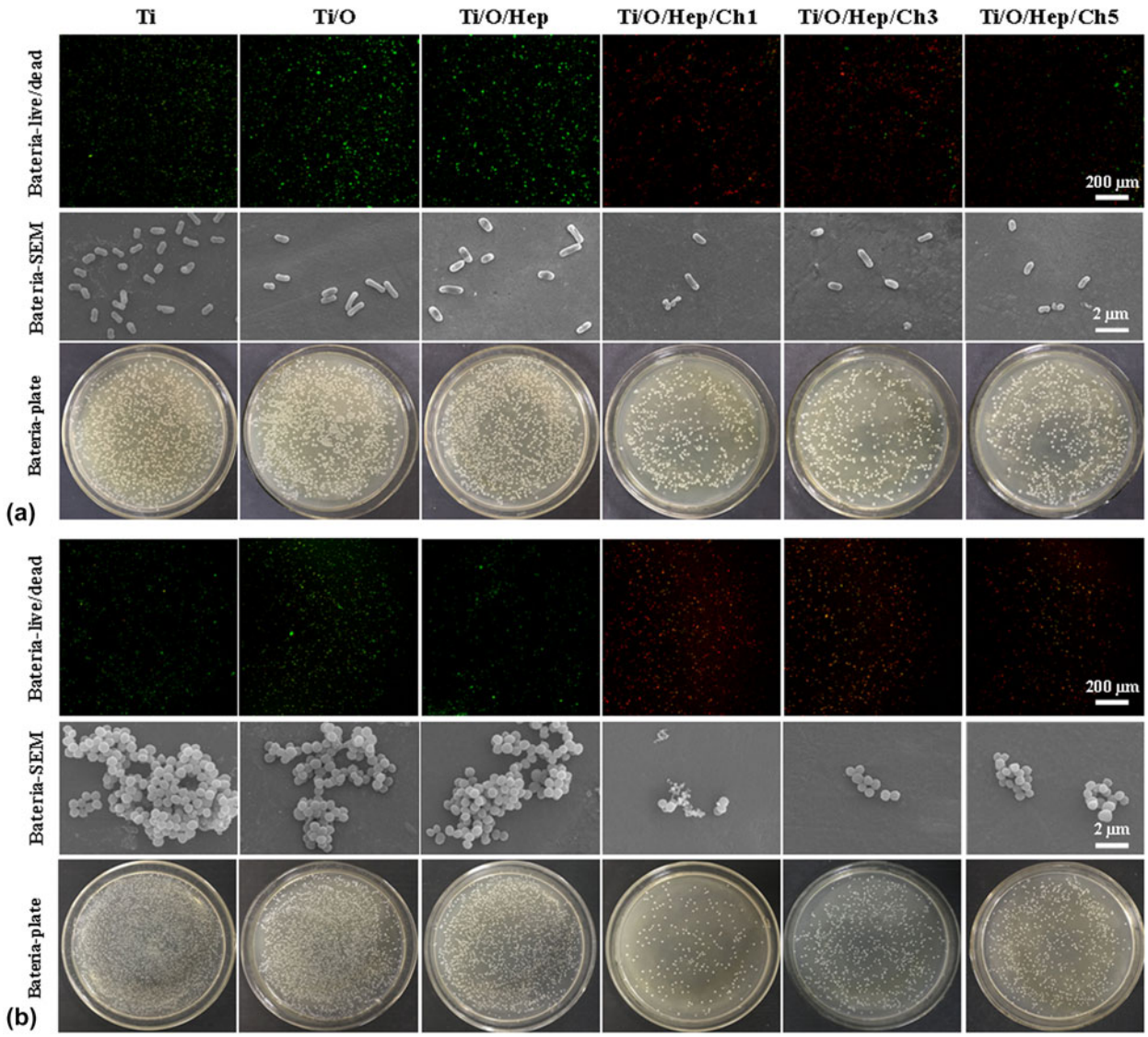


Figure 5: Antibacterial experiments: Representative fluorescence images, SEM images, and representative colony forming of (a) *E. coli* and (b) *S. aureus*.

aureus, chitosan is adsorbed on the surface of bacteria to form a layer of polymer membrane, which prevents the transport of nutrients into cells and achieves sterilization effect [24].

Biocompatibility test

No cytotoxic to endothelial cells (ECs) is one of the most important attributes of an antithrombotic implant material, since the lining of blood vessels was composed of ECs [35]. Figure 6(a) shows the fluorescence of ECs adhered on the surfaces of different samples. The results show that cells proliferated over time and there was no significant difference between the treated samples with pure Ti after 3 and 5 days. After 5 days, there was a significant growth in the number of cells, and the entire surface of all the test pieces was basically full of green living cells. The 3-(4,5-dimethylthiazol-2-yl)-2,5-diphenyl tetrazolium bromide (MTT) results [Fig. 6(b)] show that the number of cells on Ti/O/Hep/Ch1, Ti/O/Hep/Ch3, and Ti/O/Hep/Ch5 was more than Ti, Ti/O, and Ti/O/Hep after 3 and 5 days of culturing. Especially for Ti/O/Hep/Ch1, the cells show higher fluorescent intensity than those on other samples, demonstrating the better biocompatibility. The reason for this is that chitosan possesses good hydrophilicity and a positive charge, promoting cell adhesion and proliferation [36].

Conclusions

In this study, we found a simple, rapid, and efficient method to immobilize sodium heparin and CMCS on the surface of pure Ti via chemical bonding and electrostatic bonding. Initial annealing treatment builds a bridge between the heparin and

https://doi.org/10.1557/jmr.2019.358 Published online by Cambridge University Press

© Materials Research Society 2019

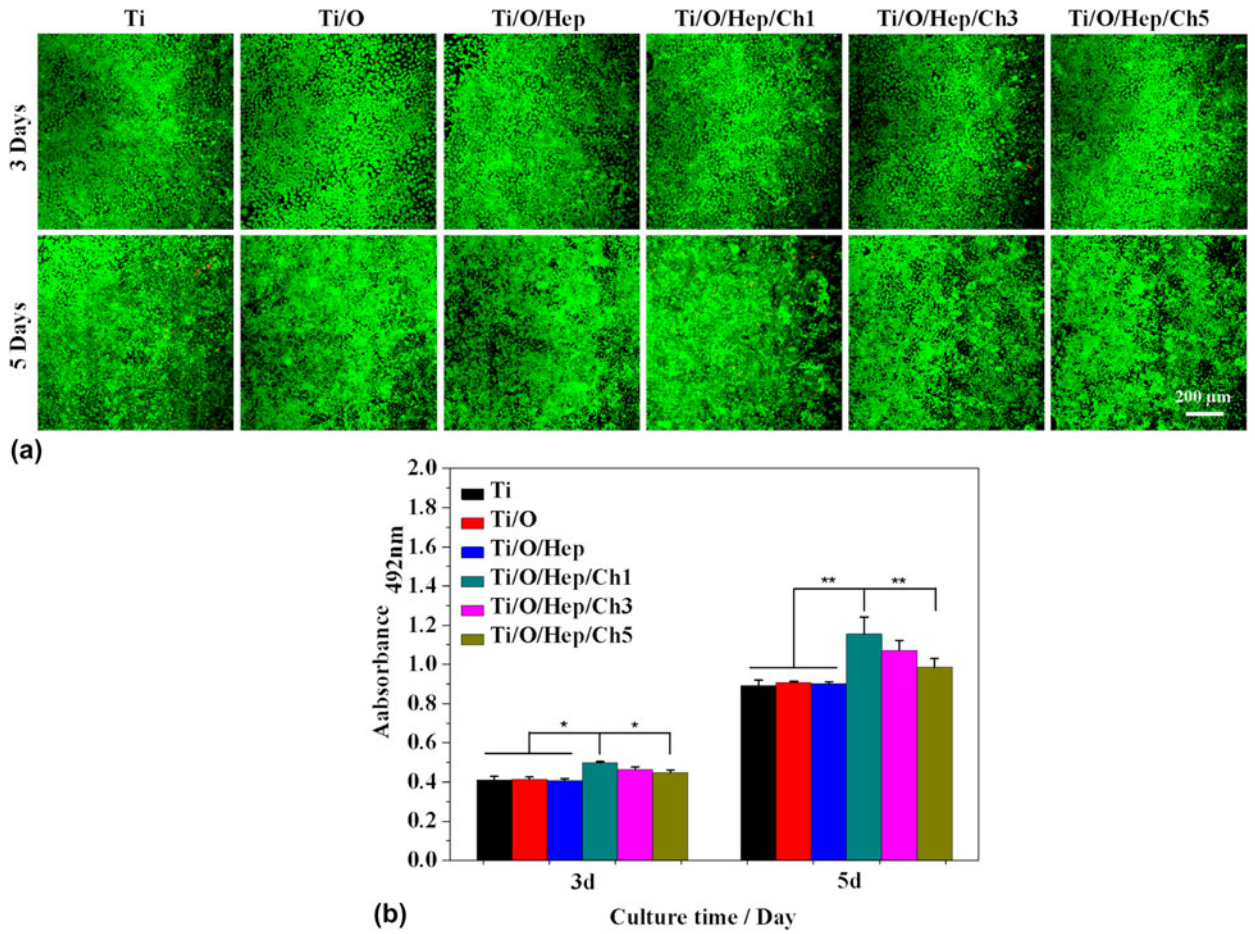


Figure 6: Biocompatibility test: (a) Fluorescence images of ECs on samples; (b) MTT results of ECs on samples. (*$P < 0.1$)

Ti, followed by immobilizing chitosan on the heparinized surfaces. The surface-functionalized Ti achieved thrombore-sistant properties, demonstrated by an inhibition of platelet adhesion, and prolonged clotting time. In addition, the mod-ified surfaces exhibited excellent antibacterial properties and the antibacterial rates against *E. coli* and *S. aureus* were, respectively, 56.5 and 74.5%. This approach is therefore believed to have great potential for the surface modification of various biomedical devices, to achieve antithrombogenic and antibacterial properties.

Material and methods

Materials

Heparin sodium injection (2 mL:12,500 unit) was produced by Tianjin Bio-Chemical Pharmaceutical Co. Ltd., China. CMCS was produced by Pure Chemistry Scientific Inc., USA. TB, paraformaldehyde (PFA), sodium dodecyl sulfate (SDS), bovine serum albumin (BSA), and FITC-labeled phalloidin were pro-duced by Sigma-Aldrich, USA. Fetal bovine serum (FBS), Dulbecco's modified Eagle medium (DMEM), penicillin–streptomycin (P/S), and PBS were produced by Gibco BRL, USA. *n*-Hexane was produced by AccuStandard Inc., USA. Beef extract and peptone were produced by Sangon Biotech, China.

Annealing treatment

Samples of Pure Ti having a diameter of 14 mm and a thickness of 2 mm were cut from a Ti rod. The surface of samples was polished with 180 ## to 2000 ## SiC sandpaper successively, then ultrasonically washed with acetone, absolute ethanol, and deionized water for 5 minutes. The Ti plates were put in the muffle furnace and were kept warm for 2 hours at 500 °C, then the Ti plates were removed after cooling in the muffle furnace, rinsed with deionized water, and blown dry in air. The samples were designated as Ti/O.

The Ti/O samples were immersed in the 40-times diluted heparin sodium solution at 37 °C in a water-bath pot for 1 h. Then, the samples were removed and rinsed with deionized water. The samples were designated as Ti/O/Hep. Afterward, the Ti/O/Hep was immersed in CMCS solution (5 g/L) for 1 h at 37 °C. Then, remove the samples and rinse with deionized

https://doi.org/10.1557/jmr.2019.358 Published online by Cambridge University Press

© Materials Research Society 2019

water. The samples were designated as Ti/O/Hep/Ch1. Other conditions remain unchanged, and the soaking time was adjusted to 20 and 12 min in the two solutions. Afterward, it was repeated for three and five times, respectively. The samples were designated as Ti/O/Hep/Ch3 and Ti/O/Hep/Ch5.

Sample characterization

A scanning electron microscope (FE-SEM; JSM-7001F, JEOL, Japan) was used to observe the morphology of the samples surface. The surface roughness was examined by atomic force microscopy (AFM; XE-100, Park Systems). The surface hydrophilicity was analyzed by the sessile drop method on the Rame'-Hart instrument (USA). The surface composition was measured with X-ray photoelectron spectroscopy (XPS; Thermo).

Heparin test

The amount of heparin immobilized was determined by the TB method. In short, the samples were immersed in 3 mL PBS, and afterward, 2 mL TB solution (0.005%, 0.01 mol/L HCl, 0.2% NaCl) was added. Then, the samples were shaken for 2 hours at 37 °C and 3 mL *n*-hexane was added. After that, the mixed solution was shaken violently for 1 min. The samples were taken out of the solution and the absorbance was measured at 630 nm. The amount of adsorbed heparin was counted in the light of the standard curve of heparin solution with different concentrations. We followed the same procedure as a blank control group and did not detect heparin levels.

To determine the shelf life, the samples were immersed in PBS at 37 °C for 10 and 20 days, and the amount of residual heparin was measured.

Protein adsorption

The samples were put into 24-well plates, 1 mL of DMEM containing 10% FBS was dropped onto samples and then incubated at 37 °C for 4 h. Then, the samples were rinsed with PBS and removed to new 24-well plates. Afterward, 500 μL SDS (1%) solution was pipetted onto each sample and then shaken for 1 h at 37 °C to collect the protein. The content of adsorbed protein in the samples was detected by an assay kit (cat# P0009; Beyotime).

In vitro antithrombogenic evaluation

Platelet adhesion

The platelet adhesion properties of the samples were assessed using fresh human whole blood. All the human whole blood was drawn from healthy adult volunteers according to ethics rules. The experiment was carried out within 12 h after the blood donation. The collected blood and 0.109 M sodium citrate were placed in a centrifuge tube at a ratio of 4:1. In order to obtain the platelet-rich plasma (PRP), whole blood was centrifuged at 1500 rpm for 15 min. Afterward, the supernatant plasma-containing platelets were collected into another centrifuge tube, and then, further centrifuged at 1500 for 15 min to get PRP. After that, 50 μL PRP was dropped onto samples and incubated for 1 h at 37 °C. Then, the samples were washed three times with PBS and fixed platelet with 3% glutaraldehyde solution for 1.5 h. To dehydrate, the samples were immersed in ethanol of different concentration gradients (20, 40, 60, 80, 90, and 100%) for 15 min. Then, the samples were dried in air for 45 min and gold-sputtered to observe the platelet morphology under a FE-SEM.

Whole blood clotting

After 50 μL of whole blood introduced onto samples, the specimens were weighed. Then, the samples were incubated for 10 min at 37 °C and moved to a beaker containing 10 mL distilled water for 10 min at 37 °C. After that, the samples covered with coagulated blood were taken out, dried, and weighed again, and the remaining solution is tested for absorbance at 540 nm.

Antibacterial activities tests

The antibacterial activity of samples against Gram-negative *E. coli* and Gram-positive *S. aureus* bacteria was assessed.

In order to stay sterile, the samples were immersed in medical alcohol for 1 h. Then, the alcohol on the samples was washed with PBS and transferred the samples to 24-well plates, and 60 μL of diluted bacterial suspension (10^4 CFU/mL) was added to the surface of each sample. Afterward, the bacteria on the samples were cultured at 37 °C for 24 h.

Fluorescence microscopy

After the bacteria were cultured for 24 h, 50 μL of stains (acridine orange/propidium iodide) were added to the surface of the samples to stain the attached bacteria. After stained for 15 min in the dark, photographs of the survival of adherent bacteria on the surface of samples were collected by fluorescence microscopy.

SEM observation

In order to fix the bacteria on the sample surface, the samples cultured with bacteria were washed with PBS and fixed with 3% glutaraldehyde solution for 1.5 h. To dehydrate, the samples were immersed in 20, 40, 60, 80, 90, and 100% sequential ethanol for 15 min. Afterward, the samples were dried in air for

https://doi.org/10.1557/jmr.2019.358 Published online by Cambridge University Press

© Materials Research Society 2019

45 min and gold-sputtered to observe the bacteria morphology under a FE-SEM.

Plate-counting method

Bacteria adhered to samples in 24-well plates were uniformly sprayed with 950 μL of PBS. Then, 80 μL diluted bacterial suspension was added to a standard agar culture medium and kept at 37 °C for 24 h. Finally, the pictures of bacterial colonies were collected. The antibacterial ratio was calculated according to the following formula: antibacterial rate (%) = $[(\beta_0 - \beta_1)/\beta_0] \times 100\%$, in which β_0 is the bacterial colonies on Ti and β_1 is the bacterial colonies on Ti/O/Hep/Ch1, Ti/O/Hep/Ch3, and Ti/O/Hep/Ch5.

In vitro biocompatibility

The ECs were cultured in DMEM supplemented with 10% FBS, 1% penicillin, and streptomycin at 37 °C in an atmosphere of 5% CO_2 and 95% air.

In order to test the toxicity of the samples, a Live/Dead staining kit was used to observe the survival of the cells on the surface of the samples. After the cells were incubated on the surface of the samples for 3 and 5 days, the samples were rinsed with PBS, and 50 mL of staining solution was added to the surface of each sample and incubated for 1 h in the dark. Afterward, the green living cells and red dead cells were investigated by confocal laser scanning microscopy (CLSM).

Cell proliferation was evaluated quantitatively with the MTT assay. After the cells were cultured for 3 and 5 days on the surface of the samples, the samples were rinsed with PBS. 1 mL of mixed solution (900 μL culture medium, 100 μL of 5 mg/mL MTT) were added to samples and cultured for 4 h. Then, the mixed solution was removed and the crystals were dissolved in 1 mL of dimethylsulfoxide (DMSO). The optical density (OD) of the solution was measured at 490 nm on a microplate reader.

Statistical analysis

Experimental data were analyzed using the one-way ANOVA. Statistical significance was considered as having $^*P < 0.05$. All experiments data were presented as the mean ± SD and were performed in triplicate.

Acknowledgments

This work was supported by the National Natural Science Foundation of China (31700834 and 51671140), Major Projects in Research and Development of Shanxi (Projects of International Cooperation, 201803D421090), the Fund for Shanxi "1331 Project" Key Innovative Research Team (1331KIRT), and Projects of Health and Family Planning Commission in Shanxi (2017066).

References

1. **J. Hasan, R.J. Crawford, and E.P. Ivanova**: Antibacterial surfaces: The quest for a new generation of biomaterials. *Trends Biotechnol.* **31**, 295 (2013).
2. **A. de los Santos Pereira, S. Sheikh, C. Blaszykowski, O. Pop-Georgievski, K. Fedorov, M. Thompson, and C. Rodriguez-Emmenegger**: Antifouling polymer brushes displaying antithrombogenic surface properties. *Biomacromolecules* **17**, 1179 (2016).
3. **S. Murugesan, J. Xie, and R.J. Linhardt**: Immobilization of heparin: Approaches and applications. *Curr. Top. Med. Chem.* **8**, 80 (2008).
4. **J.M. Goddard and J.H. Hotchkiss**: Polymer surface modification for the attachment of bioactive compounds. *Prog. Polym. Sci.* **32**, 698 (2007).
5. **K.S. Masters**: Covalent growth factor immobilization strategies for tissue repair and regeneration. *Macromol. Biosci.* **11**, 1149 (2011).
6. **H. Lee, J. Rho, and P.B. Messersmith**: Facile conjugation of biomolecules onto surfaces via mussel adhesive protein inspired coatings. *Adv. Mater.* **21**, 431 (2009).
7. **D. Aydin and S. Kizilel**: P2X7 receptor antagonist delivery vehicle based on photocrosslinked amphiphilic hybrid gels. *RSC Adv.* **8**, 18216 (2018).
8. **S. Wu, Z. Weng, X. Liu, K.W.K. Yeung, and P.K. Chu**: Functionalized TiO_2 based nanomaterials for biomedical applications. *Adv. Funct. Mater.* **24**, 5464 (2015).
9. **B. Dinan, D. Gallego-Perez, H. Lee, D. Hansford, and S.A. Akbar**: Thermally grown TiO_2, nanowires to improve cell growth and proliferation on titanium based materials. *Ceram. Int.* **39**, 5949 (2013).
10. **M. Geetha, A.K. Singh, R. Asokamani, and A.K. Gogia**: Ti based biomaterials, the ultimate choice for orthopaedic implants—A review. *Prog. Mater. Sci.* **54**, 397 (2009).
11. **S. Wu, X. Liu, K.W.K. Yeung, C. Liu, and X. Yang**: Biomimetic porous scaffolds for bone tissue engineering. *Mater. Sci. Eng., R* **80**, 1 (2014).
12. **X.J. He, G.N. Zhang, X. Wang, R.Q. Hang, X.B. Huang, L. Qin, B. Tang, and X.Y. Zhang**: Biocompatibility, corrosion resistance and antibacterial activity of TiO_2/CuO coating on titanium. *Ceram. Int.* **43**, 16185 (2017).
13. **A. Ghosh**: Effect of rolling mode and annealing temperature on microstructure and texture of commercially pure-titanium. *Mater. Charact.* **125**, 83 (2017).
14. **A. Rendón-Rivera, J.A. Toledo-Antonio, M.A. Cortés-Jácome, and C. Angeles-Chávez**: Generation of highly reactive OH groups at the surface of TiO_2, nanotubes. *Catal. Today* **166**, 18 (2011).

https://doi.org/10.1557/jmr.2019.358 Published online by Cambridge University Press

© Materials Research Society 2019

15. **D.W. Liu, P. Xiao, Y.H. Zhang, B.B. Garcia, Q.F. Zhang, Q. Guo, R. Champion, and G.Z. Cao**: TiO_2 nanotube arrays annealed in N_2 for efficient lithium-ion intercalation. *J. Phys. Chem. C* **112**, 11175 (2008).
16. **T. Fujino, M. Katayama, K. Inudzuka, T. Okuno, and K. Oura**: Surface hydroxyl formation on vacuum-annealed TiO_2(110) TiO_2(110). *Appl. Phys. Lett.* **79**, 2716 (2001).
17. **C. Arrouvel, M. Digne, M. Breysse, H. Toulhoat, and P. Raybaud**: Effects of morphology on surface hydroxyl concentration: A DFT comparison of anatase–TiO_2, and γ-alumina catalytic supports. *J. Catal.* **222**, 152 (2004).
18. **P. Sie, F. Ofosu, F. Fernandez, M.R. Buchanan, M. Petitou, and B. Boneu**: Respective role of antithrombin III and heparin cofactor II in the in vitro anticoagulant effect of heparin and of various sulphated polysaccharides. *Br. J. Haematol.* **64**, 707 (1986).
19. **R.D. Rosenberg and P.S. Damus**: The purification and mechanism of action of human antithrombin-heparin cofactor. *J. Biol. Chem.* **248**, 6490 (1973).
20. **E.W. Salzman, R.D. Rosenberg, M.H. Smith, J.N. Lindon, and L. Favreau**: Effect of heparin and heparin fractions on platelet aggregation. *J. Clin. Invest.* **65**, 64 (1980).
21. **R.A. Muzzarelli**: Biomedical exploitation of chitin and chitosan via mechano-chemical disassembly, electrospinning, dissolution in imidazolium ionic liquids, and supercritical drying. *Mar. Drugs* **9**, 1510 (2011).
22. **L. Hu, Y. Sun, and Y. Wu**: Advances in chitosan-based drug delivery vehicles. *Nanoscale* **5**, 3103 (2013).
23. **M.S. Benhabiles, R. Salah, H. Lounici, N. Drouiche, G. Mfa, and N. Mameri**: Antibacterial activity of chitin, chitosan and its oligomers prepared from shrimp shell waste. *Food Hydrocolloids* **29**, 48 (2012).
24. **E.I. Rabea, M.E. Badawy, C.V. Stevens, G. Smagghe, and W. Steurbaut**: Chitosan as antimicrobial agent: Applications and mode of action. *Biomacromolecules* **4**, 1457 (2003).
25. **L. Upadhyaya, J. Singh, V. Agarwal, and R.P. Tewari**: The implications of recent advances in carboxymethyl chitosan based targeted drug delivery and tissue engineering applications. *J. Controlled Release* **186**, 54 (2014).
26. **R. Raftery, F.J. O'Brien, and S.A. Cryan**: Chitosan for gene delivery and orthopedic tissue engineering applications. *Molecules* **18**, 5611 (2013).
27. **P.V. Asharani, G.L.K. Mun, M.P. Hande, and S. Valiyaveettil**: Cytotoxicity and genotoxicity of silver nanoparticles in human cells. *ACS Nano* **85**, 743 (2011).
28. **J.P. Piret, D. Jacques, J.N. Audinot, J. Mejia, E. Boilan, F. Noël, M. Fransolet, C. Demazy, S. Lucas, C. Saout, and O. Toussaint**: Copper(II) oxide nanoparticles penetrate into HepG2 cells, exert cytotoxicity via oxidative stress and induce pro-inflammatory response. *Nanoscale* **4**, 7168 (2012).
29. **A.S. Antonio, L.S.M. Wiedemann, and V.F.V. Junior**: The genus capsicum: A phytochemical review of bioactive secondary metabolite. *RSC Adv.* **8**, 25767 (2018).
30. **F.J. Xu, Y.L. Li, E.T. Kang, and K.G. Neoh**: Heparin-coupled poly(poly(ethylene glycol) monomethacrylate)–Si(111) hybrids and their blood compatible surfaces. *Biomacromolecules* **6**, 1759 (2005).
31. **C. Cheng, S. Sun, and C. Zhao**: Progress in heparin and heparin-like/mimicking polymer-functionalized biomedical membranes. *J. Mater. Chem. B* **2**, 7649 (2014).
32. **P. Le Thi, Y. Lee, H.J. Kwon, K.M. Park, M.H. Lee, J-C. Park, and K.D. Park**: Tyrosinase-mediated surface coimmobilization of heparin and silver nanoparticles for antithrombotic and antimicrobial activities. *ACS Appl. Mater. Interfaces* **9**, 20376 (2017).
33. **B. Sivaraman and R.A. Latour**: The relationship between platelet adhesion on surfaces and the structure versus the amount of adsorbed fibrinogen. *Biomaterials* **31**, 832 (2010).
34. **X.L. Liu, L. Yuan, D. Li, Z.C. Tang, Y.W. Wang, G.J. Chen, H. Chen, and J.L. Brash**: Blood compatible materials: State of the art. *J. Mater. Chem. B* **2**, 5718 (2014).
35. **Y.Q. Chen, X. Zhang, S. Zhao, M.F. Maitz, W.T. Zhang, S. Yang, J.L. Mao, N. Huang, and G.J. Wan**: In situ incorporation of heparin/bivalirudin into a phytic acid coating on biodegradable magnesium with improved anticorrosion and biocompatible properties. *J. Mater. Chem. B* **5**, 4162 (2017).
36. **S. Wang, C. Sun, S. Guan, W. Li, J. Xu, D. Ge, M. Zhuang, T. Liu, and X. Ma**: Chitosan/gelatin porous scaffolds assembled with conductive poly(3,4-ethylenedioxythiophene) nanoparticles for neural tissue engineering. *J. Mater. Chem. B* **5**, 4774 (2017).

https://doi.org/10.1557/jmr.2019.358 Published online by Cambridge University Press

© Materials Research Society 2019